HHS Public Access

Author manuscript

Cell Transplant. Author manuscript; available in PMC 2016 March 28.

Published in final edited form as:

Cell Transplant. 2015 ; 24(1): 115–131. doi:10.3727/096368913X674657.

Permissive Schwann Cell Graft/Spinal Cord Interfaces for Axon Regeneration

Ryan R. Williams[*], **Martha Henao**[*], **Damien D. Pearse**[*,†], and **Mary Bartlett Bunge**[*,†,‡]

[*]

[†]

[‡]

Abstract

The transplantation of autologous Schwann cells (SCs) to repair the injured spinal cord is currently being evaluated in a clinical trial. In support, this study determined properties of spinal cord/SC bridge interfaces that enabled regenerated brainstem axons to cross them, possibly leading to improvement in rat hindlimb movement Fluid bridges of SCs and Matrigel were placed in complete spinal cord transections. Compared to pregelled bridges of SCs and Matrigel, they improved regeneration of brainstem axons across the rostral interface. The regenerating brainstem axons formed synaptophysin^{+} bouton-like terminals and contacted MAP2A^{+} dendrites at the caudal interface. Brainstem axon regeneration was directly associated with glial fibrillary acidic protein (GFAP^{+}) astrocyte processes that elongated into the SC bridge. Electron microscopy revealed that axons, SCs, and astrocytes were enclosed together within tunnels bounded by a continuous basal lamina. Neuroglycan (NG2) expression was associated with these tunnels. One week after injury, the GFAP^{+} processes coexpressed nestin and brain lipid-binding protein, and the tips of GFAP^{+}/NG2^{+} processes extended into the bridges together with the regenerating brainstem axons. Both brainstem axon regeneration and number of GFAP^{+} processes in the bridges correlated with improvement in hindlimb locomotion. Following SCI, astrocytes may enter a reactive state that prohibits axon regeneration. Elongation of astrocyte processes into SC bridges, however, and formation of NG2^{+} tunnels enable brainstem axon regeneration and improvement in function. It is important for spinal cord repair to define conditions that favor elongation of astrocytes into lesions/transplants.

Keywords

Spinal cord injury; Schwann cells (SCs); Astrocytes; Neuroglycan (NG2); Axon regeneration; Transplantation; Interface

Address correspondence to Mary Bartlett Bunge, Ph.D., The Miami Project to Cure Paralysis, Lois Pope Life Center, PO Box 016960, R-48, Miami, FL, 33101, USA. Tel: +1-305-243-4596; Fax: +1-305-243-3923; MBunge@miami.edu.

The authors declare no conflicts of interest.

INTRODUCTION

Injury to the spinal cord results in scar and cavity formation at the lesion site. The scar is composed of basal lamina sheets, a tight meshwork of interwoven astrocyte processes (4,5) and numerous growth-inhibitory components (22,26,66) that function to wall off the lesion and protect uninjured tissue from secondary damage (11,59,68). Although numerous cell transplantation strategies have been developed to nullify the deleterious lesion environment (72), scar tissue at the interface impedes axon regeneration both into (25) and out of these grafts (76), thereby limiting functional recovery. Interestingly, some astrocytes are permissive for axonal growth when they elongate linearly oriented processes into the lesion (45,75) or transplant (14,20) site. Thus, the reaction of astrocytes that are situated at the interface between a cell transplant and the spinal cord parenchyma contributes to the propensity for successful repair.

The transplantation of Schwann cells (SCs), prepared from autologous peripheral nerve, for human central nervous system (CNS) repair was first proposed by Bunge (8), and this strategy is now being evaluated clinically (www.clinicaltrials.gov; NCT01739023). Early landmark transplantation strategies that demonstrated successful regeneration of CNS axons utilized peripheral nerve grafts implanted acutely after complete spinal cord transection (37,61). In this rigorous model of spinal cord injury (SCI), these peripheral nerve grafts (62), as well as polymer channels containing a purified population of SCs (79,81), promoted intraspinal but not supraspinal axon regeneration. Supraspinal axons regenerated into SC transplants, however, when additional treatments were introduced (13,27,30,31,55,56,58,80). Utilizing combination strategies, these early studies reported modest improvements in function, although no morphological evidence of synapses across the site of injury was shown.

More recently, Fouad and colleagues (27) slightly modified SC bridge preparation by transplanting SCs in fluid Matrigel® that subsequently gelled upon reaching body temperature. This method differed from other studies because SC bridges previously had been gelled before transplantation. When Fouad and colleagues (27) utilized initially fluid bridges in combination with additional treatments, they reported a relatively robust improvement in hindlimb locomotion after complete transection injury. Therefore, we sought to determine if the transplantation of an initially fluid SC bridge alone is sufficient to improve the capacity for repair.

We report here that the acute transplantation of SCs in fluid Matrigel into sites of complete transection SCI, without any additional treatments, promotes regeneration of brainstem axons and that they form bouton-like terminals at the caudal interface. Analysis of the host spinal cord/SC bridge interfaces revealed that astrocyte processes elongated in association with SCs and regenerated axons, sometimes in neuroglycan-positive ($NG2^+$) tunnels. Brainstem axons did not enter the SC bridge when the astrocytes failed to extend processes into the bridge and formed a sharp rather than irregular border. Both the numbers of regenerated axons and glial fibrillary acidic protein positive ($GFAP^+$) processes in the bridge correlated with improvement in hindlimb movement.

MATERIALS AND METHODS

Experimental Design

The experimental design and methods used in this study were described in detail previously by Williams and colleagues (77). Briefly, young adult (postnatal day 35) female Fischer rats, all bom on the same day, were obtained from Harlan Laboratories (Frederick, MD, USA). Each rat received two separate surgeries: first, stereotaxic (Narishige International USA, Inc., East Meadow, NY, USA) injection of serotype 2 AAV-EGFP (adeno-associated virus containing enhanced green fluorescent protein) to anterogradely label brainstem axons and, second, complete transection of the spinal cord with implantation of a SC bridge. Each stereotaxic surgery took approximately 90–100 min, so only two rats were injected with AAV-EGFP vectors per day. In order to achieve maximal transgene expression at the time of injury, all stereotaxic surgeries were performed between 2 and 6 weeks before injury. Thus, the postnatal age of the rats ranged from 6 to 10 weeks on the day they were injected with AAV-EGFP vectors. The second surgery, the complete transection of the spinal cord and implantation of a SC bridge, took 20–25 min. To ensure that all the rats were the same age at the time of injury, these surgeries were performed over the course of 2 days. In this way, the rats were 12 weeks of age and weighed approximately 160–180 g at the time of injury. Then, either 1 or 6 weeks following transection and transplantation, the rats were perfused for histological analysis. All surgical procedures and analyses were performed blinded to the experimental group. All procedures were conducted in accordance with animal welfare standards established by the USA National Institutes of Health Guide for the Care and Use of Laboratory Animals, as well as the Institutional Animal Care and Use Committee at the University of Miami Miller School of Medicine.

AAV Vectors

Serotype 2 AAV vectors were generated by the Miami Project to Cure Paralysis Viral Vector Core, using the AAV Helper-Free System from Stratagene (La Jolla, CA, USA). The transgene plasmid for enhanced EGFP was kindly provided by Dr. Scott Whittemore (University of Louisville, KY, USA). The AAV-EGFP used in this study contained 2.4×10^{10} genomes/ml and had a functional titer of 2.6×10^{8} TU/ml.

Stereotaxic Injection of AAV

Detailed stereotaxic coordinates and injection procedures were described previously by Williams and colleagues (77). Briefly, while anesthetized, stereotaxic injections were performed bilaterally to target descending brainstem populations in the locus coeruleus, ventrolateral pons, and the ventromedial rostral medulla. Each animal was injected with 19 µl of AAV, at a rate of 0.25 µl per minute, using an sp310i syringe pump (World Precision Instruments, Sarasota, FL, USA) together with a 5-µl syringe modified with a 5-cm 33-gauge needle (Hamilton Company, Reno, NV, USA).

Generation of Purified SCs

Purified (95–98%) SC populations were obtained from adult female Fischer rat sciatic nerves as described previously (49,51). Following purification, SCs were passaged to

confluency three times and resuspended in Dulbecco's modified Eagle's medium (DMEM; Invitrogen, Grand Island, NY, USA) for transplantation.

Spinal Cord Transection and SC Bridge Transplantation

While anesthetized, the rats received a laminectomy from thoracic vertebrae levels 7 (T7) to T9, with significant lateral exposure, and the dorsal roots were cut. Then a single incision was made with angled microscissors (Fine Science Tools, Foster City, CA, USA) to completely transect the spinal cord at T8. The ventral dura was severed, the ventral roots were cut, and the spinal cord stumps retracted to create a 2–3-mm gap. Completeness of the transection was confirmed by lifting the rostral and caudal stumps and placing them into a 5.0-mm-long polyacrylonitrile/polyvinyl chloride (PAN/PVC) channel, kindly provided by Dr. Patrick Tresco (University of Utah, Salt Lake City, UT, USA). Then, 3.0×10^6 SCs in 15 µl DMEM were mixed with 10 µl of Matrigel (BD Biosciences, San Jose, CA, USA) and injected through the rostral of two holes previously created in the top of the channel (27,77). Matrigel has been found to improve transplanted SC survival (54). This fluid mixture then gelled rapidly upon exposure to the animal's body temperature. Pregelled bridges were prepared by mixing 3.0×10^6 SCs in 15 µl DMEM with 10 µl of Matrigel and inserting this mixture via one end of the same size polymer channel (without holes). These bridges were allowed to solidify for 20 min in the incubator before positioning in the transection gap. Following the surgery, the rats received subcutaneous injections of 5 ml physiological saline twice a day (bis in die; BID) for 7 days, gentamicin (5 mg/kg; APP Pharmaceuticals, Schaumburg, IL, USA) once a day (quaque die; QD) for 7 days to prevent urinary tract infection, buprenorphine (0.1 mg/kg; Reckitt Benckiser Pharmaceuticals, Richmond, VA, USA) three times a day (ter in die; TJD) for 3 days to reduce discomfort, and bladder expression manually BID until micturition returned. Two animals were housed per cage starting a week after transplantation; no rehabilitation was performed [except for Basso, Beattie and Bresnahan (BBB) scoring]. In animal Set A, two animal groups compared initially fluid ($n = 7$) to initially pregelled ($n = 7$) Matrigel/SC bridges. Set B ($n = 1$) received only initially fluid SC bridges to further characterize outgrowth of astrocyte processes and brainstem axons.

Tissue Processing, Immunohistochemistry, Electron Microscopy, and Imaging

The rats received terminal anesthesia (200 mg/kg ketamine; Vedco, St. Joseph, MO, USA, and 20 mg/kg xylazine; Acorn, Decatur, IL, USA). Their left ventricles were injected with 20 USP units of heparin (Sigma, St. Louis, MO, USA), and they were subjected to transcardial perfusion with 200 ml 4°C, phosphate-buffered saline (PBS; Invitrogen) followed by 400 ml 4°C, 4% paraformaldehyde (PFA; Sigma) in 0.1 M phosphate buffer (pH 7.4; Sigma). Spinal cords were extirpated and further fixed in PFA overnight and cryoprotected in PBS plus 30% sucrose and 0.025% sodium azide (all Sigma). Tissue blocks were embedded in PBS plus 12% gelatin (Sigma) and 0.025% sodium azide and quickly frozen in crushed dry ice. The SC bridges with attached rostral and caudal spinal cord were sectioned parasagittally from left to right at 20 µm using a cryostat (Leica, Buffalo Grove, IL, USA) and mounted directly onto a series of five slides (Surgipath, Buffalo Grove, IL, USA). In this way, sections were mounted onto a slide series at 100-µm intervals.

The antigenic sites were blocked in PBS with 0.5% Triton-X (Sigma) plus 5.0% normal goat serum (Atlanta Biological, Lawrenceville, GA, USA) and/or 5.0% normal donkey serum (Atlanta Biological). Then, tissue sections were incubated overnight with one or more of the following primary antibodies: GFP (chicken, 3.19 mg/ml, 1:500; Chemicon, Temecula, CA, USA), dopamine -hydroxylase (D H; mouse, 1:500; Chemicon), 5-hydroxytryptophan (5-HT; rabbit, 1:2,000; ImmunoStar, Hudson, WI, USA), GFAP (SMI 22; mouse, 1:500; Covance, Denver, PA, USA; rabbit, 1:500; DAKO, Carpinteria, CA, USA), S100 (rabbit, 1:500; DAKO), nestin (mouse, 1:500; Abcam, Cambridge, MA, USA), NG2 (rabbit, 1:200; Chemicon), brain lipid-binding protein (BLBP; rabbit, 1:200; Chemicon), low-affinity nerve growth factor receptor (p75; mouse, 1:2, hybridoma 192-IgG; American Type Culture Collection, Manassas, VA, USA), synaptophysin (rabbit, 1:500; DAKO), microtubule-associated protein 2A (MAP2A; mouse, 1:200; Chemicon), together with secondary antibodies conjugated to 488 or 594 fluorophores (1:200; Molecular Probes, Eugene, OR, USA), as well as 0.1% Hoechst dye solution (10 mM, Sigma) to label nuclei. All images of immunostaining were obtained with an Olympus FV1000 confocal microscope (Center Valley, PA, USA).

Tissue for electron microscopic analysis was prepared as described previously (49,81). Briefly, following overnight fixation in 4% PFA, SC bridge tissue was cut transversely into 1-mm slices from the rostral to the caudal interfaces. These slices were further fixed in 2% buffered glutaraldehyde (Sigma) followed by 1% osmium tetroxide (Electron Microscopy Sciences, Fort Washington, PA, USA) and embedded in Epon Araldite (Electron Microscopy Sciences). Thin sections stained with uranyl acetate (Electron Microscopy Sciences) and lead citrate (Electron Microscopy Sciences) were imaged on a Philips CM10 electron microscope (FEI, Hillsboro, OR, USA).

Quantification of Axon Regeneration and GFAP$^+$ Processes

Adhering to guidelines established for the assessment of axon regeneration (69), parasagittal sections of the SC bridge were analyzed by a line-transect method (Fig. 1) using Neurolucida (MBF Bioscience, Williston, VT, USA) and an Axiophot fluorescent microscope (Zeiss, Thornwood, NY, USA) and MAC 5000 XYZ stage (Ludl, Hawthorne, NY, USA). The extent of host spinal cord tissue inside the polymer channel was defined by the expression of GFAP$^+$ astrocyte somata at the spinal cord/SC bridge interfaces. The zero point, 0, was determined on the tissue sections that contained the tips of rostral and caudal spinal cord inserted farthest into the polymer channel, respectively. This distance from the ends of the polymer channel was then used to locate 0 on the remaining sections. Then, using Hoechst staining to visualize the tissue, dorsoventral lines were drawn on each section along the rostrocaudal axis at −10.0 mm, 0.25 mm, 0.5 mm, 1.0 mm, 1.5 mm, 2.0 mm, and 2.5 mm from 0, as well as 0.25 mm, 0.5 mm, and 1.0 mm from 0. The length of these lines at a given location indicated the dorsoventral thickness of bridge tissue. By focusing up and down through the entire tissue section, the number of axons and GFAP$^+$ processes that crossed a given dorsoventral line was quantified. In this way, a transverse plane of tissue was analyzed, and the area was determined by multiplying the tissue section thickness (20 μm) by the length of the dorsoventral lines at a given location. To normalize for differences

in the amount of bridge tissue sampled across animals, this area was used to report counts per square millimeter.

Assessment of Hindlimb Locomotor Function

To assess hindlimb motor function, animals were subjected to a 4-rnin open-field BBB locomotor test (3). All rats were tested 1 week before the stereotaxic injection surgery and 1 week before the transection/bridge transplantation. Their bladders were expressed prior to testing. The rats were then tested on a weekly basis, for 6 weeks after the transection/bridge transplantation. In the final week, the rats also were recorded with a video camera while being tested.

Statistics

All statistical analyses were performed with the Graph Pad Prism 5 software (La Jolla, CA, USA). GFP^+ axon regeneration and $GFAP^+$ processes were quantified from 14 experimental animals. Those with initially fluid bridges (n=7) were compared to those with pregelled bridges (n = 7) and analyzed using a two-way ANOVA with a Bonferroni post hoc test Error bars or ± indicate the SEM. A second group of animals (n = 11) was transplanted with initially fluid bridges and used to determine one-tailed, nonparametric correlations between $GFAP^+$ processes, axon regeneration, and BBB test scores.

RESULTS

Two sets of animals were prepared. Set A directly compared animals receiving either fluid or pregelled SC bridges. Set B consisted of animals receiving only fluid SC bridges to further characterize extension of astrocyte processes and brainstem axons into the bridge.

The Acute Transplantation of SCs and Initially Fluid Matrigel After Complete Spinal Cord Transection Improve the Interface for Axonal Regeneration Compared to Pregelled Transplants

Our previous studies of complete spinal cord transection injuries found that the implantation of Matrigel alone (in control animals) promoted negligible regeneration of axons into the bridge (81), so this experimental group was not included in the present experiments. The combination of SCs and pregelled Matrigel, however, promoted intra-, but not supraspinal, axons to regenerate (81). To determine if the fluidity of an acutely transplanted matrix directly influences brainstem axon regeneration, initially fluid bridges, of SCs and Matrigel were compared to pregelled bridges (animal Set A). As described previously (77), brainstem neurons were anterogradely labeled with AAV-EGFP to easily visualize regeneration of their axons. In the current study, brainstem axons regenerated into both types of transplants, although fewer brainstem axons grew into the pregelled bridges (Fig. 2A) compared to the initially fluid bridges (Fig. 2B). These differences were quantified utilizing the line-transect method (Fig. 1). At all measured distances from the rostral interface (0.25 mm, 0.5 mm, and 1.0 mm), more brainstem axons regenerated into the initially fluid than pregelled bridges (p< 0.001, two-way ANOVA) (Fig. 2C). An average of 229 ± 35 EGFP-labeled brainstem axons/mm^2 were found to regenerate 0.25 mm into the initially fluid SC bridges compared to an average of only 68 ± 4 axons/mm^2 in the pregelled bridges. The Bonferroni post hoc

analysis identified the most significant difference between initially fluid and pregelled bridges to be at 0.25 ram from the rostral interface (Fig. 2C). This suggests that differences in the bridges may pertain more to the interfaces that form rather than axonal growth within the bridge.

When the morphology of astrocytes was analyzed using GFAP immunohistochemistry, $GFAP^+$ astrocytes at the interfaces formed either sharp or irregular boundaries in both initially fluid and pregelled bridges. Most of the interfaces in the pregelled bridges, however, exhibited a glial scar-like morphology with a sharp boundary of dense $GFAP^+$ processes that did not enter the bridge (Fig. 2A). In contrast, interfaces in the initially fluid bridges were mostly irregular, and long $GFAP^+$ processes extended into the transplant (Fig. 2B). In order to quantify these differences, the line-transect method was utilized to analyze the number of these $GFAP^+$ processes entering the SC bridge. At all measured distances from both the rostral and caudal interfaces, initially fluid bridges exhibited a greater than 10-fold increase in the number of $GFAP^+$ processes entering the SC bridge compared to animals that received pregelled bridges ($p < 0.0001$, two-way ANOVA) (Fig. 2D). In summary, compared to pregelled SC bridges, initially fluid bridges create interfaces that better support brainstem axon regeneration into the bridge.

The Acute Transplantation of SCs and Matrigel Enables Brainstem Axon Regeneration Across a Site of Complete Spinal Cord Transection

In the initially fluid bridges of SCs and Matrigel, brainstem axons not only regenerated into the transplant but also crossed the entire lesion site and reached the distal interface (Fig. 3). The $EGFP^+$ axons regenerated through the rostral host spinal cord/SC bridge interface in regions where $GFAP^+$ processes entered the bridge (Fig. 3A–C). These astrocytes coexpressed GFAP and S100 and were easily distinguished from SCs that only expressed S100. The $EGFP^+$ axons, usually oriented parallel to the longitudinal axis of the polymer channel, regenerated beyond $GFAP^+$ processes that entered the bridge from the rostral interface. Most $EGFP^+$ axons and astrocyte processes were found in the peripheral and ventral regions of the polymer channel, similar to the highest densities of SC myelination previously reported by Xu et al. (81). Several brainstem populations were targeted by the stereotaxic injections of AAV-EGFP (77), including vestibular, noradrenergic, serotonergic, and reticular nuclei. This resulted in a heterogeneous population of EGFP-labeled brainstem axons regenerating into the bridge, with varied morphologies and beaded labeling. The EGFP-labeled brainstem axons were often observed in association with SCs and sometimes found in close proximity to autofluorescent macrophages (stars, Fig. 3B, D). In some animals, more than 100 $EGFP^+$ brainstem axons extended at least 2.5 mm, often reaching the caudal interface (Fig. 3D).

In animal Set B (that received only initially fluid SC bridges), the rostral interfaces were further characterized. In addition to $EGFP^+$ brainstem axons, D H^+ noradrenergic axons (Fig. 4A), and 5-HT^+ serotonergic axons (Fig. 4B) regenerated into the bridge; some of these $5HT^+$ and DBH^+ axons also expressed EGFP. The regenerating axons entered the bridge with $GFAP^+$ astrocyte processes. The astrocyte processes typically entered the bridge in an aligned, longitudinal orientation, extending parallel to axons, and in close proximity to

S100$^+$/GFAP$^-$ SCs (Fig. 4C, D). The GFAP$^+$ processes, SCs, and EGFP$^+$ brainstem axons were often bundled together as a trio. Confocal analysis of tissue section *z*-planes revealed that this trio remained bundled together across the entire interface, with the axons primarily located in the middle of the bundle (Fig. 4E). Furthermore, electron microscopy images showed that the trio was contained within a continuous basal lamina surrounded by longitudinally oriented collagen fibrils and fibroblasts (Fig. 5). The basal lamina appeared to provide a tunnel reminiscent of a band of Bungner in regenerating peripheral nerve.

The elongation of GFAP$^+$ processes and the regeneration of EGFP$^+$ brainstem axons were quantified in animal Set B using the line-transect method (Fig. 1). GFAP$^+$ processes were found at all measured locations across the bridge but were diminished near the middle. A direct correlation was observed between the number of GFAP$^+$ processes/mm^2 at 0.25 mm past the rostral interface and the number of EGFP$^+$ axons/mm^2 that regenerated 0.25 mm ($p < 0.005$, $r^2 = 0.31$) (Fig. 6A), 0.5 mm ($p< 0.005$, $r^2 = 0.33$) (Fig. 6B), 1.0 mm ($p<0.05$, $r^2 = 0.24$) (Fig. 6C), and 1.5 mm ($p<0.05$, $r^2 = 0.38$) (Fig. 6D). Thus, when more GFAP$^+$ processes elongate into the SC bridge from the rostral interface, more EGFP$^+$ axons are able to regenerate into the bridge. We conclude that the elongation of GFAP$^+$ astrocyte processes into a transplant defines that interface as permissive for the regeneration of brainstem axons.

SCs and Elongated GFAP$^+$ Processes Associate With NG2$^+$ Tunnels

To examine early interface formation between the spinal cord parenchyma and the initially fluid SC bridges, additional animals were perfused 1 week after transplantation. At this time, reactive astrocytes, as defined by increased expression of GFAP, were found to elongate processes into the SC transplants. These astrocytes also expressed markers of immature glia, nestin, and BLBP (Fig. 7). As with levels of GFAP expression, the number of cells coexpressing nestin decreased with distance from the interface. Numerous nestrn$^+$/GFAP$^-$ cells appeared to form a wave emanating from the spinal cord stumps into the bridge. In the middle of the bridge, the linear arrays of nestin$^+$/GFAP$^-$ cells were likely SCs.

One week after transection, EGFP$^+$ brainstem axons were found to regenerate into regions of NG2 expression. NG2$^+$/GFAP$^+$ processes formed tunnels through which the axons traversed the acutely injured interface, often in close proximity to macrophages (Fig. 8). The NG2 expression was typically exterior to the GFAP and EGFP expression (Fig. 8E, F), as if outside the basal larnina that enclosed the trio of axons, SCs, and astrocyte processes (Fig. 4). The tips of regenerating brainstem axons were in close association with the tips of the NG2$^+$/GFAP$^+$ processes (Fig. 8G, H). Confocal analysis of tissue section *z*-planes revealed that the tips of EGFP$^+$ brainstem axons and NG2$^+$/GFAP$^+$ processes twisted around one another as they extended across the interface.

By six weeks after transplantation of initially fluid Matrigel and SCs into a site of complete transection, robust and linear NG2 expression was present throughout the bridge (Fig. 9), not unlike that found after injury of peripheral nerves (60). In the middle of the bridge, NG2 was likely produced by SCs based on coexpression with p75 (Fig. 9B). The expression of NG2 did not appear to impede axon regeneration, as EGFP$^+$ brainstem axons were found in close proximity to NG2 throughout the entire bridge. Thus, after transplantation, SCs associate with GFAP$^+$ processes and NG2$^+$ tunnels, enabling brainstem axon regeneration.

Brainstem Axons Form Bouton-Like Terminals at the Caudal Interface

In the initially fluid transplants, both the rostral and caudal spinal cord/SC bridge interfaces revealed a highly interdigitated $GFAP^+$ border. Similar numbers of $GFAP^+$ processes extended from either interface (Fig. 2D). Nevertheless, clearly intact, regenerating $EGFP^+$ descending brainstem axons were not observed to cross the caudal interface and enter the caudal spinal cord. Instead, when $EGFP^+$ axons reached the caudal interface, they either extended between the interdigitations of astrocytes and were closely associated with them or were deflected away to grow in another direction (Fig. 3D).

Brainstem axons that regenerated to the caudal interface and were closely associated with astrocyte processes formed bouton-like terminals, identifiable due to the anterograde transport of EGFP to the distal tips (Fig. 10). To further characterize these structures, the expression of synaptophysin was assessed using confocal microscopy (Fig. 10A–F). At the caudal interface, synaptophysin was expressed as distinct puncta, typically less than 0.5 μm in diameter. When brainstem axons formed bouton-like structures in association with $GFAP^+$ processes, the $synaptophysin^+$ puncta were often colocalized within the $EGFP^+$ terminals. Furthermore, some astrocyte processes that extended into the SC bridge from the caudal spinal cord were associated with $MAP2A^+$ dendrites. When brainstem axons regenerated to the caudal interface and formed $EGFP^+$ bouton-like terminals, they were in close proximity to these dendrites (Fig. 10G–J). In summary, $EGFP^+$ axons that regenerated to the caudal interface and formed bouton-like terminals expressed synaptophysin and closely associated with both $GFAP^+$ astrocyte processes and $MAP2A^+$ dendrites.

Both Brainstem Axon Regeneration and the Elongation of $GFAP^+$ Processes Are Associated With Improved Hindlimb Movement

Following complete transection and transplantation of SCs and Matrigel, the animals exhibited progressive hindlimb improvement in an open field, as assessed by BBB scoring. A direct comparison of the scores between pregelled and initially fluid bridges in Set A did not reveal a statistically significant difference. However, in Set B animals implanted with initially fluid bridges, there was a direct correlation between the number of $EGFP^+$ brainstem axons that reached the caudal interface and week 6 BBB scores ($p < 0.05$, $r^2 = 0.22$) (Fig. 11A). There was also a direct correlation between the number of $GFAP^+$ processes/mm^2 that elongated into the SC transplant and week six BBB scores ($p < 0.05$, $r^2 = 0.3$) (Fig. 11B). Thus, the presence of elongated $GFAP^+$ astrocyte processes may be used to determine if a SC transplant supports improvement in hindlimb movement.

DISCUSSION

The Transplantation of SCs Promotes Brainstem Axon Regeneration After SCI

Whereas previous work found supraspinal axons to regenerate only when a SC bridge was combined with additional treatments (6), the current study demonstrates that the transplantation of a SC bridge alone promotes brainstem axon regeneration. Two differences in this study and previous investigations of the SC bridge were i) brainstem axon regeneration was easily visualized using AAV-EGFP as an anterograde tracer (77) and ii) some SC bridges were not pregelled prior to transplantation. Compared to pregelled bridges

of SCs and Matrigel, this study demonstrated that initially fluid bridges promote both a robust increase in the elongation of astrocyte processes as well as the regeneration of brainstem axons into the transplant Early work with collagen matrices reported limited axon regeneration into pregelled compared to initially fluid transplants (36). The advantage of initially fluid transplants over pregelled ones may be i) in pregelled SC bridges, components in Matrigel, such as collagen type IV and laminin, may self-assemble into basal lamina (73) before transplantation and thereby contribute to a mesh-work of astrocyte processes similar to the glial limitans (23,24,40), and ii) fluid mixtures may rapidly conform to the surface of the cord stumps, thereby limiting the invasion of meningeal fibroblasts and inflammatory cells, analogous to duraplasty (30,31,82). The invasion of meningeal cells and their interaction with astrocytes creates glial limitans-like structures that may impede axonal growth (33,39,65).

The Elongation of GFAP$^+$ Processes Defines an Interface as Permissive for Brainstem Axon Regeneration and Functional Improvement

After complete transection/SC bridge transplantation, numerous astrocyte processes entered the bridge and were associated with both brainstem axon regeneration and improvement in hmdlimb movement. After CNS injury, reactive astrocytes are often inhibitory to axon regeneration and recovery of function (22,66), although they also exert many beneficial functions (68). Early studies of complete transections reported axons sprouting short distances into the lesion in association with astrocytes (32,45). These sprouts were often found with endogenous SCs and, together with axons, were enclosed within a continuous basal lamina (7,44), similar to the current study. These tunnel-like structures are distinct from the inhibitory sheets of basal lamina found in CNS scar tissue (4,5). Axons often grow in association with astrocytes during development (67,75) and following the transplantation of various grafts into the CNS (14,34,38), including SCs (13,30,31,80,82). Astrocytes extend processes into SC grafts with the administration of glial-derived neurotrophic factor (20), and transplants of glial precursor-derived astrocytes cultured with bone morphogenetic protein extend processes and promote axon regeneration (15). The current study supports these findings and demonstrates that the quantification of elongated GFAP$^+$ processes may be used to determine if a CNS–graft interface is permissive for axon regeneration and functional improvement Accordingly, the presence of elongated astrocyte processes should be assessed in any scaffold and/or cellular transplantation therapy designed to treat SCI.

After SCI, astrocytes enter a reactive state as defined by their increased expression of GFAP and/or proliferation to create new astrocytes. New astrocytes also may be generated by ependymal cells and/or NG2$^+$ progenitors (2,29,44,48,52,84,85). In the current study, astrocyte processes at the interface expressed nestin and BLBP 1 week after SC transplantation, indicating they were in a more immature-like state. The processes resembled those of type II fibrous astrocytes and, given their expression of developmental proteins, may be derived from dedifferentiating and/or de novo astrocytes. Immature astrocytes express numerous developmental proteins that support axonal growth (41,53,74). The astrocytes at the interface expressed markers of miniature glia, irrespective of their morphology (i.e., if they elongated processes into the bridge or formed a tight meshwork that walled off the transplant). However, brainstem axons only regenerated across regions of

the interface where astrocytes expressing markers of immature glia also elongated processes into the transplant. Given that glial morphology alone may not be sufficient for growth (16,17), the data presented here suggest that morphology dictates the potential for axon regeneration if and when an appropriate balance of growth and inhibitory proteins are expressed (35,46), that is, if the glia are expressing developmental proteins. In this way, the elongation of astrocyte processes across transplant interfaces likely establishes three-dimensional structures that determine how regenerating axons become exposed to the myriad of growth-promoting and inhibitory cues.

GFAP$^+$ Processes and Axons Elongate in Association With SCs and NG2$^+$ Tunnels

Elongated GFAP$^+$ processes associated with transplanted SCs in NG2$^+$ tunnels escorted regenerating brainstem into the bridge. NG2 may be derived from numerous cellular sources, including progenitor cells, astrocytes, and SCs (12,18,35,43,47,48,78). In addition, NG2$^+$ pericytes that associate with blood vessels (35,47) may enable brainstem axon regeneration, analogous to sensory axon regeneration along blood vessels after injury of the dorsal roots (28). Although direct contact with purified NG2 inhibits axonal growth (71), axonal growth after SCI is observed in regions of NG2 expression (18,35,43,47), and NG2$^+$ progenitor cells protect axons from macrophage-induced dieback (9,10). In the current study, GFAP$^+$/NG2$^+$ processes also appeared to protect regenerating axons from macrophages as they crossed the interface. In addition, the transplanted SCs and GFAP$^+$ processes may enable brainstem axons to regenerate by mediating the spatial and temporal localization of NG2.

Astrocyte processes, SCs, and regenerating axons were observed to be bundled together within tunnels of basal lamina. Whereas NG2 expression appeared to be exterior to the axons in the bundles, the precise localization of NG2 with respect to the basal lamina remains to be determined. NG2 may be membrane bound or deposited after cleavage. Macrophage-produced matrix metallopeptidase 9 (MMP-9) may cleave membrane-bound NG2 (9,42), whereas astrocyte processes that elongate into the bridge may limit cleavage/deposition by expressing tissue inhibitor of metalloproteinase-1 (TIMP-1) (50). Given that brainstem axons appear to grow together with the tips of NG2$^+$ processes, either membrane bound or cleavage deposits of NG2 (1) may prevent the subsequent regeneration of axons through the tunnels and/or provide guidance. Thus, there may be a temporal limit to the permissivity of NG2$^+$ tunnels. Such temporal changes may partially explain the failure of regenerating brainstem axons to enter the caudal spinal cord (76). Alternatively, the regenerating axons may stop growing because they form bouton-like terminals.

Brainstem Axons Regenerate to the Caudal SC Graft Interface, Form Bouton-Like Terminals, and Are Associated With Improvement in HindLimb Movements

Following the complete transection of the thoracic spinal cord, the transplantation of SCs promoted the regeneration of brainstem axons across the entire lesion site. Regenerating brainstem axons that reached the caudal interface formed bouton-like terminals. Synaptophysin expression was often colocalized as puncta with the bouton-like terminals. Furthermore, the bouton-like terminals were associated with MAP2A$^+$ dendrites and astrocyte processes that entered the SC bridge from the caudal spinal cord. Finally, the

number of brainstem axons that reached the caudal interface was directly correlated with improvement in hindlimb movement. Together, this suggests that the regeneration of brainstem axons across the entire SC bridge may mediate behavioral improvement through interaction with neurons adjacent to the caudal interface.

Numerous studies have reported behavioral improvement following treatment of complete transections, and this is at least in part mediated by synaptic rearrangements of the central pattern generator (CPG) (19,63). Following complete transection, regenerating axons conduct action potentials across the SC bridge (57), motor-evoked potentials (MEPs) recover after implantation of oligodendrocyte progenitors and/or motor neuron progenitors (21), and transcranial brainstem stimulation induces MEPs following transplantation of olfactory ensheathing glia (70). New synapses, however, may not be necessary as evoked potentials can be elicited by the extrasynaptic release of neurotransmitters (64), and improvement in hindlimb movement may then be mediated by propriospinal neurons that relay to the CPG (83). Therefore, brainstem axons that regenerate across the SC bridge and reach the caudal interface may mediate improvement in hindlimb movement through extrasynaptic release of neurotransmitter and/or the potential formation of synapses at the caudal SC bridge–spinal cord interface.

In conclusion, this study supports the clinical use of SCs for SCI repair and defines important characteristics of permissive spinal cord/graft interfaces. We demonstrated that the elongation of astrocyte processes into SC transplants and formation of $NG2^+$ tunnels enables brainstem axon regeneration and improvement in function. Therefore, it is important for spinal cord repair to understand conditions that favor astrocytes to be permissive for axonal growth into lesions/transplants.

Acknowledgments

The authors are grateful to the Viral Vector Core and the Animal Core facilities at the Miami Project to Cure Paralysis for providing the AAV-EGFP vectors and animal care, respectively; Alison Moody and Margaret Bates for help with immunohistochemistry and electron microscopy; and Drs. Patrick Wood James Guest, Brian Noga, and Ian Hentall for their discussion and/or critical reading of this manuscript. This work was supported by NINDS grants 09923 (M.B.B.) and 056281 (D.D.P. and M.B.B.), the Miami Project to Cure Paralysis, the Buoniconti Fund to Cure Paralysis, and the Christine E. Lynn Distinguished Professorship in Neuroscience (M.B.B.).

References

1. Asher RA, Morgenstern DA, Properzi F, Nishiyama A, Levine JM, Fawcett JW. Two separate metalloproteinase activities are responsible for the shedding and processing of the NG2 proteoglycan in vitro. Mol Cell Neurosci. 2005; 29:82–96. [PubMed: 15866049]
2. Barnabé-Heider F, Göritz C, Sabelström H, Takebayashi H, Pfrieger FW, Meletis K, Frisén J. Origin of new glial cells in intact and injured adult spinal cord. Cell Stem Cell. 2010; 7:470–482. [PubMed: 20887953]
3. Basso DM, Beattie MS, Bresnahan JC. Graded histological and locomotor outcomes after spinal cord contusion using the NYU weight-drop device versus transection. Exp Neurol. 1996; 139:244–256. [PubMed: 8654527]
4. Bernstein JJ, Getz R, Jefferson M, Kelemen M. Astrocytes secrete basal lamina after hemisection of rat spinal cord. Brain Res. 1985; 327:135–141. [PubMed: 3986496]
5. Brightman MW. The brain's interstitial clefts and their glial walls. J Neurocytol. 2002; 31:595–603. [PubMed: 14501201]

6. Bunge MB. Novel combination strategies to repair the injured mammalian spinal cord. J Spinal Cord Med. 2008; 31:262–269. [PubMed: 18795474]
7. Bunge MB, Holets VR, Bates ML, Clarke TS, Watson BD. Characterization of photochemically induced spinal cord injury in the rat by light and electron microscopy. Exp Neurol. 1994; 127:76–93. [PubMed: 8200439]
8. Bunge, RP. Changing use of nerve tissue culture 1950–1975. In: Tower, DB., editor. The nervous system, volume one: The basic neurosciences. New York, NY: Raven Press; 1975. p. 31-42.
9. Busch SA, Hamilton JA, Horn KP, Cuascut FX, Cutrone R, Lehman N, Deans RJ, Ting AE, Mays RW, Silver J. Multipotent adult progenitor cells prevent macrophage-mediated axonal dieback and promote regrowth after spinal cord injury. J Neurosci. 2011; 31:944–953. [PubMed: 21248119]
10. Busch SA, Horn KP, Cuascut FX, Hawthorne AL, Bai L, Miller RH, Silver J. Adult NG2+ cells are permissive to neurite outgrowth and stabilize sensory axons during macrophage-induced axonal dieback after spinal cord injury. J Neurosci. 2010; 30:255–265. [PubMed: 20053907]
11. Bush TG, Puvanachandra N, Homer CH, Polito A, Ostenfeld T, Svendsen CN, Mucke L, Johnson MH, Sofroniew MV. Leukocyte infiltration, neuronal degeneration, and neurite outgrowth after ablation of scar-forming, reactive astrocytes in adult transgenic mice. Neuron. 1999; 23:297–308. [PubMed: 10399936]
12. Buss A, Pech K, Kakulas BA, Martin D, Schoenen J, Noth J, Brook G. NG2 and phosphacan are present in the astroglial scar after human traumatic spinal cord injury. BMC Neurol. 2009; 9:32. [PubMed: 19604403]
13. Chen A, Xu XM, Kleitman N, Bunge MB. Methylprednisolone administration improves axonal regeneration into Schwann cell grafts in transected adult rat thoracic spinal cord. Exp Neurol. 1996; 138:261–276. [PubMed: 8620925]
14. Davies JE, Huang C, Proschel C, Noble M, Mayer-Proschel M, Davies SJ. Astrocytes derived from glial-restricted precursors promote spinal cord repair. J Biol. 2006; 5:7. [PubMed: 16643674]
15. Davies JE, Pröschel C, Zhang N, Noble M, Mayer-Pröschel M, Davies SJ. Transplanted astrocytes derived from BMP- or CNTF-treated glial-restricted precursors have opposite effects on recovery and allodynia after spinal cord injury. J Biol. 2008; 7:24. [PubMed: 18803859]
16. Davies SJ, Field PM, Raisman G. Regeneration of cut adult axons fails even in the presence of continuous aligned glial pathways. Exp Neurol. 1996; 142:203–216. [PubMed: 8934554]
17. Davies SJ, Fitch MT, Memberg SP, Hall AK, Raisman G, Silver J. Regeneration of adult axons in white matter tracts of the central nervous system. Nature. 1997; 390:680–683. [PubMed: 9414159]
18. de Castro R Jr, Tajrishi R, Claros J, Stallcup WB. Differential responses of spinal axons to transection: Influence of the NG2 proteoglycan. Exp Neurol. 2005; 192:299–309. [PubMed: 15755547]
19. de Leon RD, Roy RR, Edgerton VR. Is the recovery of stepping following spinal cord injury mediated by modifying existing neural pathways or by generating new pathways? A perspective. Phys Ther. 2001; 81:1904–1911. [PubMed: 11736625]
20. Deng LX, Hu J, Liu N, Wang X, Smith GM, Wen X, Xu XM. GDNF modifies reactive astrogliosis allowing robust axonal regeneration through Schwann cell-seeded guidance channels after spinal cord injury. Exp Neurol. 2011; 229:238–250. [PubMed: 21316362]
21. Erceg S, Ronaghi M, Oria M, Rosello MG, Arago MAP, Lopez MG, Radojevic I, Moreno-Manzano V, Rodriguez-Jimenez FJ, Bhattacharya SS, Cordoba J, Stojkovic M. Transplanted oligodenrocytes and motoneuron progenitors generated from human embryonic stem cells promote locomotor recovery after spinal cord transection. Stem Cells. 2010; 28:1541–1549. [PubMed: 20665739]
22. Fawcett JW, Asher RA. The glial scar and central nervous system repair. Brain Res Bull. 1999; 49:377–391. [PubMed: 10483914]
23. Feringa ER, Kowalski TF, Vahlsing HL. Basal lamina formation at the site of spinal cord transection. Ann Neurol. 1980; 8:148–154. [PubMed: 6448569]
24. Feringa ER, Vahlsing HL, Woodward M. Basal lamina at the site of spinal cord transection in the rat: An ultrastructural study. Neurosci Lett. 1984; 51:303–308. [PubMed: 6521958]
25. Fishman PS, Nilaver G, Kelly JP. Astrogliosis limits the integration of peripheral nerve grafts into the spinal cord. Brain Res. 1983; 277:175–180. [PubMed: 6640291]

26. Fitch MT, Silver J. CNS injury, glial scars, and inflammation: Inhibitory extracellular matrices and regeneration failure. Exp Neurol. 2008; 209:294–301. [PubMed: 17617407]
27. Fouad K, Schnell L, Bunge MB, Schwab ME, Liebscher T, Pearse DD. Combining Schwann cell bridges and olfactory-ensheathing glia grafts with chondroitinase promotes locomotor recovery after complete transection of the spinal cord. J Neurosci. 2005; 25:1169–1178. [PubMed: 15689553]
28. Fraher JP. The transitional zone and CNS regeneration. J Anat. 2000; 196:137–158. [PubMed: 10697296]
29. Frisén J, Johansson CB, Török C, Risling M, Lendahl U. Rapid, widespread, and longlasting induction of nestin contributes to the generation of glial scar tissue after CNS injury. J Cell Biol. 1995; 131:453–464. [PubMed: 7593171]
30. Guest JD, Hess D, Schnell L, Schwab ME, Bunge MB, Bunge RP. Influence of IN-1 antibody and acidic FGF-fibrin glue on the response of injured corticospinal tract axons to human Schwann cell grafts. J Neurosci Res. 1997; 50:888–905. [PubMed: 9418975]
31. Guest JD, Rao A, Olson L, Bunge MB, Bunge RP. The ability of human Schwann cell grafts to promote regeneration in the transected nude rat spinal cord. Exp Neurol. 1997; 148:502–522. [PubMed: 9417829]
32. Guth L, Barrett CP, Donati EJ, Deshpande SS, Albuquerque EX. Histopathological reactions an axonal regeneration in the transected spinal cord of Hibernating squirrels. J Comp Neurol. 1981; 203:297–308. [PubMed: 7309924]
33. Hermanns S, Klapka N, Müller HW. The collagenous lesion scar—An obstacle for axonal regeneration in brain and spinal cord injury. Restor Neurol Neurosci. 2001; 19:139–148. [PubMed: 12082234]
34. Hurtado A, Cregg JM, Wang HB, Wendell DF, Oudega M, Gilbert RJ, McDonald JW. Robust CNS regeneration after complete spinal cord transection using aligned poly-L-lactic acid microfibers. Biomaterials. 2011; 32:6068–6079. [PubMed: 21636129]
35. Jones LL, Sajed D, Tuszynski MH. Axonal regeneration through regions of chondroitin sulfate proteoglycan deposition after spinal cord injury: A balance of permissiveness and inhibition. J Neurosci. 2003; 23:9276–9288. [PubMed: 14561854]
36. Joosten EA, Bär PR, Gispen WH. Collagen implants and corticospinal axonal growth after mid-thoracic spinal cord lesion in the adult rat. J Neurosci Res. 1995; 41:481–490. [PubMed: 7473879]
37. Kao CC, Chang LW, Bloodworm JM Jr. Axonal regeneration across transected mammalian spinal cords: An electron microscopic study of delayed microsurgical nerve grafting. Exp Neurol. 1977; 54:591–615. [PubMed: 844527]
38. Kawaja MD, Gage FH. Reactive astrocytes are substrates for the growth of adult CNS axons in the presence of elevated levels of nerve growth factor. Neuron. 1991; 7:1019–1030. [PubMed: 1684900]
39. Kruger S, Sievers J, Hansen C, Sadler M, Berry M. Three morphologically distinct types of interface develop between adult host and fetal brain transplants: Implications for scar formation in the adult central nervous system. J Comp Neurol. 1986; 249:103–116. [PubMed: 3755447]
40. Liesi P, Kauppila T. Induction of type IV collagen and other basement-membrane-associated proteins after spinal cord injury of the adult rat may participate in formation of the glial scar. Exp Neurol. 2002; 173:31–45. [PubMed: 11771937]
41. Liesi P, Silver J. Is astrocyte laminin involved in axon guidance in the mammalian CNS? Dev Biol. 1988; 130:774–785. [PubMed: 3143614]
42. Liu H, Shubayev VI. Matrix metalloproteinase-9 controls proliferation of NG2+ progenitor cells immediately after spinal cord injury. Exp Neurol. 2011; 231:236–246. [PubMed: 21756907]
43. Lu P, Jones LL, Tuszynski MH. Axon regeneration through scars and into sites of chronic spinal cord injury. Exp Neurol. 2007; 203:8–21. [PubMed: 17014846]
44. Matthews MA, St Onge MF, Faciane CL. An electron microscopic analysis of abnormal ependymal cell proliferation and envelopment of sprouting axons following spinal cord transection in the rat. Acta Neuropathol. 1979; 45:27–36. [PubMed: 760363]
45. Matthews MA, St Onge MF, Faciane CL, Gelderd JB. Axon sprouting into segments of rat spinal cord adjacent to the site of a previous transection. Neuropath App Neurobiol. 1979; 5:181–196.

46. McKeon RJ, Schreiber RC, Rudge JS, Silver J. Reduction of neunte outgrowth in a model of glial scarring following CNS injury is correlated with the expression of inhibitory molecules on reactive astrocytes. J Neurosci. 1991; 11:3398–3411. [PubMed: 1719160]
47. McTigue DM, Tripathi R, Wei P. NG2 colocalizes with axons and is expressed by a mixed cell population in spinal cord lesions. J Neuropathol Exp Neurol. 2006; 65:406–420. [PubMed: 16691121]
48. McTigue DM, Wei P, Stokes BT. Proliferation of NG2-positive cells and altered oligodendrocyte numbers in the contused rat spinal cord. J Neurosci. 2001; 21:3392–3400. [PubMed: 11331369]
49. Meijs MF, Timmers L, Pearse DD, Tresco PA, Bates ML, Joosten EA, Bunge MB, Oudega M. Basic fibroblast growth factor promotes neuronal survival but not behavioral recovery in the transected and Schwann cell implanted rat thoracic spinal cord. J Neurotrauma. 2004; 21:1415–1430. [PubMed: 15672632]
50. Moore CS, Milner R, Nishiyama A, Frausto RF, Serwanski DR, Pagarigan RR, Whitton JL, Miller RH, Crocker SJ. Astrocytic tissue inhibitor of metalloproteinase-1 (TIMP-1) promotes oligodendrocyte differentiation and enhances CNS myelination. J Neurosci. 2011; 31:6247–6254. [PubMed: 21508247]
51. Morrissey TK, Kleitman N, Bunge RP. Isolation and functional characterization of Schwann cells derived from adult peripheral nerve. J Neurosci. 1991; 11:2433–2442. [PubMed: 1869923]
52. Mothe AJ, Tatar CH. Proliferation, migration, and differentiation of endogenous ependymal region stem/progenitor cells following minimal spinal cord injury in the adult rat. Neuroscience. 2005; 131:177–187. [PubMed: 15680701]
53. Müller HW, Junghans U, Kappler J. Astroglial neurotrophic and neurite-promoting factors. Pharmacol Ther. 1995; 65:1–18. [PubMed: 7716180]
54. Patel V, Joseph G, Patel A, Patel SS, Bustin D, Mawson D, Tuesta LM, Puentes R, Ghosh M, Pearse DD. Suspension matrices for improved Schwann-cell survival after implantation into the injured rat spinal cord. J Neurotrauma. 2010; 27:789–801. [PubMed: 20144012]
55. Pearse DD, Pereira FC, Marcillo AE, Bates ML, Berrocal YA, Filbin MT, Bunge MB. cAMP and Schwann cells promote axonal growth and functional recovery after spinal cord injury. Nat Med. 2004; 10:610–616. [PubMed: 15156204]
56. Pearse DD, Sanchez AR, Pereira FC, Andrade CM, Puzis R, Pressman Y, Golden K, Kitay BM, Blits B, Wood PM, Bunge MB. Transplantation of Schwann cells and/or olfactory ensheathing glia into the contused spinal cord: Survival, migration, axon association, and functional recovery. Glia. 2007; 55:976–1000. [PubMed: 17526000]
57. Pinzon A, Calancie B, Oudega M, Noga BR. Conduction of impulses by axons regenerated in a Schwann cell graft in the transected adult rat thoracic spinal cord. J Neurosci Res. 2001; 64:533–541. [PubMed: 11391708]
58. Ramón-Cueto A, Plant GW, Avila J, Bunge MB. Long-distance axonal regeneration in the transected adult rat spinal cord is promoted by olfactory ensheathing glia transplants. J Neurosci. 1998; 18:3803–3815. [PubMed: 9570810]
59. Renault-Mihara F, Okada S, Shibata S, Nakamura M, Toyama Y, Okano H. Spinal cord injury: Emerging beneficial role of reactive astrocytes' migration. Int J Biochem Cell Biol. 2008; 40:1649–1653. [PubMed: 18434236]
60. Rezajooi K, Pavlides M, Winterbottomm J, Stallcup WB, Hamlyn PJ, Lieberman AR, Anderson PN. NG2 proteoglycan expression in the peripheral nervous system: Upregulation following injury and comparison with CNS lesions. Mol Cell Neurosci. 2004; 25:572–584. [PubMed: 15080887]
61. Richardson PM, McGuinness UM, Aguayo AJ. Axons from CNS neurons regenerate into PNS grafts. Nature. 1980; 284:264–265. [PubMed: 7360259]
62. Richardson PM, McGuinness UM, Aguayo AJ. Peripheral nerve autografts to the rat spinal cord: Studies with axonal tracing methods. Brain Res. 1982; 237:147–162. [PubMed: 6176289]
63. Rossignol S, Frigon A. Recovery of locomotion after spinal cord injury: Some facts and mechanisms. Annu Rev Neurosci. 2011; 34:413–440. [PubMed: 21469957]
64. Schmidt BJ, Jordan LM. The role of serotonin in reflex modulation and locomotor rhythm production in the mammalian spinal cord. Brain Res Bull. 2000; 53:689–710. [PubMed: 11165804]

65. Shearer MC, Fawcett JW. The astrocyte/meningeal cell interface—A barrier to successful nerve regeneration? Cell Tissue Res. 2001; 305:267–273. [PubMed: 11545264]
66. Silver J, Miller JH. Regeneration beyond the glial scar. Nat Rev Neurosci. 2004; 5:146–156. [PubMed: 14735117]
67. Smith GM, Miller RH, Silver J. Changing role of forebrain astrocytes during development, regenerative failure, and induced regeneration upon transplantation. J Comp Neurol. 1986; 251:23–43. [PubMed: 3760257]
68. Sofroniew MV. Molecular dissection of reactive astrogliosis and glial scar formation. Trends Neurosci. 2009; 32:638–647. [PubMed: 19782411]
69. Steward O, Zheng B, Tessier-Lavigne M. False resurrections: Distinguishing regenerated from spared axons in the injured central nervous system. J Comp Neurol. 2003; 459:1–8. [PubMed: 12629662]
70. Takeoka A, Jindrich DL, Muñoz-Quiles C, Zhong H, van den Brand R, Pham DL, Ziegler MD, Ramon-Cueto A, Roy RR, Edgerton VR, Phelps PE. Axon regeneration can facilitate or suppress hindlimb function after olfactory ensheathing glia transplantation. J Neurosci. 2011; 31:4298–4310. [PubMed: 21411671]
71. Tan AM, Zhang W, Levine JM. NG2: A component of the glial scar that inhibits axon growth. J Anat. 2005; 207:717–725. [PubMed: 16367799]
72. Tetzlaff W, Okon EB, Karimi-Abdolrezaee S, Hill CE, Sparling JS, Plemel JR, Plune WT, Tsai EC, Baptiste D, Smithson LJ, Kawaja MD, Fehlings MG, Kwon BK. A systematic review of cellular transplantation therapies for spinal cord injury. J Neurotrauma. 2011; 28:1611–1682. [PubMed: 20146557]
73. Timpl R, Brown JC. Supramolecular assembly of basement membranes. Bioessays. 1996; 18:123–132. [PubMed: 8851045]
74. Tomaselli KJ, Neugebauer KM, Bixby JL, Lilien J, Reichardt LF. N-cadherin and integrins: Two receptor systems that mediate neuronal process outgrowth on astrocyte surfaces. Neuron. 1988; 1:33–43. [PubMed: 2856086]
75. White RE, Jakeman LB. Don't fence me in: Harnessing the beneficial roles of astrocytes for spinal cord repair. Rester Neurol Neurosci. 2008; 26:197–214.
76. Williams RR, Bunge MB. Schwann cell transplantation: A repair strategy for spinal cord injury? Functional neural transplantation III. Primary and stem cell transplantation for brain repair. Prog Brain Res. 2012; 201:295–307. [PubMed: 23186720]
77. Williams RR, Pearse DD, Tresco PA, Bunge MB. The assessment of adeno-associated viral vectors as potential intrinsic treatments for brainstem axon regeneration. J Gene Med. 2012; 14:20–34. [PubMed: 22106053]
78. Wu D, Shibuya S, Miyamoto O, Itano T, Yamamoto T. Increase of NG2-positive cells associated with radial glia following traumatic spinal cord injury in adult rats. J Neurocytol. 2005; 34:459–469. [PubMed: 16902766]
79. Xu XM, Chen A, Guénard V, Kleitman N, Bunge MB. Bridging Schwann cell transplants promote axonal regeneration from both the rostral and caudal stumps of transected adult rat spinal cord. J Neurocytol. 1997; 26:1–16. [PubMed: 9154524]
80. Xu XM, Guénard V, Kleitman N, Aebischer P, Bunge MB. A combination of BDNF and NT-3 promotes supraspinal axonal regeneration into Schwann cell grafts in adult rat thoracic spinal cord. Exp Neurol. 1995; 134:261–272. [PubMed: 7556546]
81. Xu XM, Guénard V, Kleitman M, Bunge MB. Axonal regeneration into Schwann cell-seeded guidance channels grafted into transected adult rat spinal cord. J Comp Neurol. 1995; 35:145–160. [PubMed: 7896937]
82. Xu XM, Zhang SX, Li H, Aebischer P, Bunge MB. Regrowth of axons into the distal spinal cord through a Schwann-cell-seeded mini-channel implanted into hemisected adult rat spinal cord. Eur J Neurol. 1999; 11:1723–1740.
83. Yakovenko S, Kowalczewski J, Prochazka A. Intraspinal stimulation caudal to spinal cord transections in rats. Testing the propriospinal hypothesis. J Neurophysiol. 2007; 97:2570–2574. [PubMed: 17215510]

84. Zai LJ, Wrathall JR. Cell proliferation and replacement following contusive spinal cord injury. Glia. 2005; 50:247–257. [PubMed: 15739189]

85. Zhu X, Hill RA, Nishiyama A. NG2 cells generate oligodendrocytes and gray matter astrocytes in the spinal cord. Neuron Glia Biol. 2008; 4:19–26. [PubMed: 19006598]

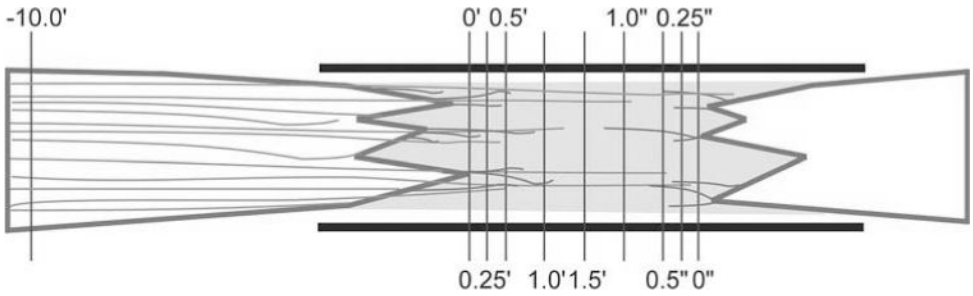

Figure 1.

An illustration of the line-transect method for quantifying axons and astrocyte processes. Enhanced green fluorescent protein-positive ($EGFP^+$) axons (green) and glial fibrillary acidic protein-positive ($GFAP^+$) processes (red) enter a SC bridge. The polymer channel (thick black lines) and the transverse lines used for quantification (thin purple lines) are diagrammed. The numbers represent rnillimeters from the rostral (0) and caudal (0) interfaces. Rostral cord left, caudal cord right, dorsal up, ventral down.

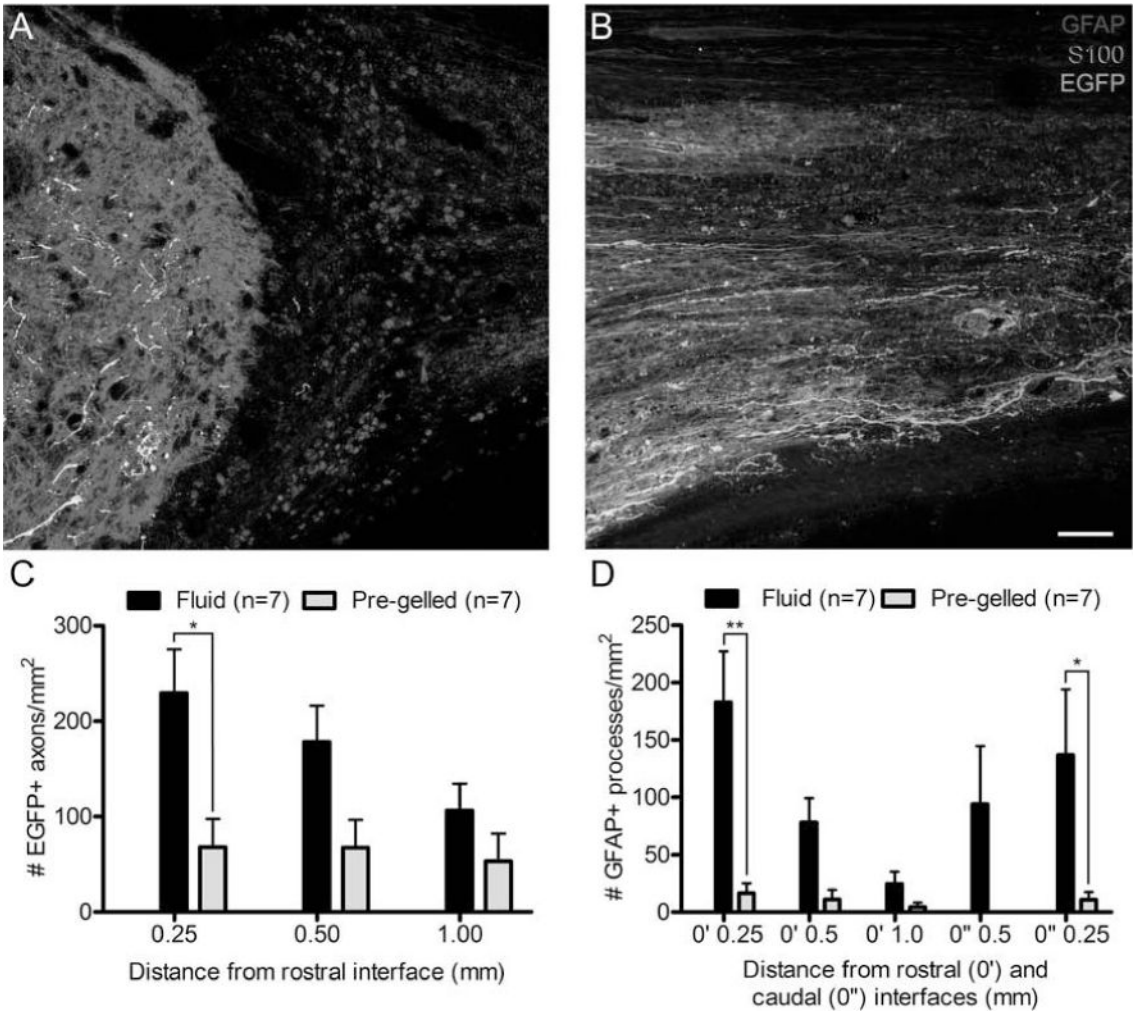

Figure 2.

Acute transplantation of an initially fluid bridge of SCs and Matrigel compared to a pregelled bridge improves the spinal cord/SC bridge interface for axonal regeneration into the bridge. (A) A rostral interface of a pregelled SC bridge shows $GFAP^+$ (red) astrocytes forming a sharp boundary with $S100^+$ (blue) SCs where few $EGFP^+$ (green) axons enter the SC bridge. Astrocytes appear pink due to their coexpression of S100 and GFAP. (B) A rostral interface of an initially fluid SC bridge shows an irregular boundary where $GFAP^+$ processes extend parallel with $S100^+$ SCs and many EGFP+ brainstem axons, into the transplant Brainstem axons are white when in close proximity to astrocytes (scale bar: 20 μm). (C) More $EGFP^+$ brainstem axons regenerate in fluid versus pregelled SC bridges (two-way ANOVA, $p < 0.001$; *Bonferroni post hoc test $p < 0.05$). (D) The number of astrocyte processes that enter from both the rostral and caudal interfaces is greater in fluid versus pregelled SC bridges (two-way ANOVA, $p < 0.0001$; **Bonferroni post hoc test $p < 0.01$; *Bonferroni post hoc test $p < 0.05$).

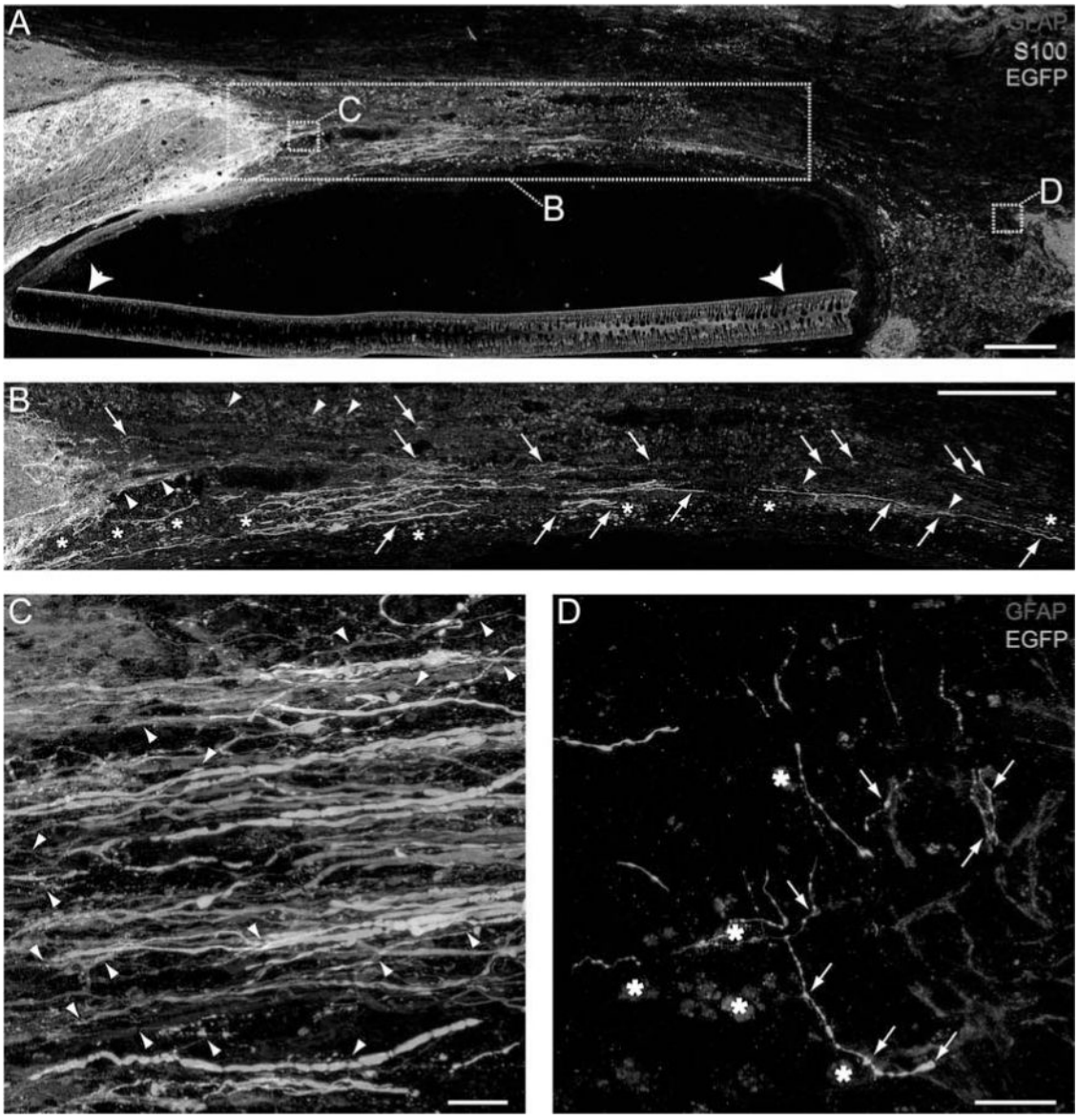

Figure 3.

The acute transplantation of SCs and Matrigel is sufficient for brainstem axons to regenerate following complete transection. (A) EGFP$^+$ (green) brainstem axons regenerate into and across an initially fluid SC (S100$^+$, blue) bridge surrounded by a polymer channel (arrowheads). GFAP$^+$ (red) astrocytes appear pink due to their coexpression of S100. Brainstem axons are white when in close proximity to astrocytes. The boxes indicate the regions of higher magnification images in the same or an adjacent section. (B) Numerous EGFP$^+$ brainstem axons (arrows) regenerate across the SC bridge. GFAP$^+$ processes (arrowheads) enter the bridge at the rostral interface (A, B, scale bars: 250 ∝m). (C) Many EGFP$^+$ brainstem axons cross the rostral spinal cord/SC bridge interface together with GFAP$^+$ processes (arrowheads). (D) EGFP$^+$ brainstem axons regenerate across the entire SC bridge and reach the caudal SC bridge/spinal cord interface. Arrows indicate regions of

close apposition between brainstem axons and astrocytes (C, D, scale bars: 10 ∝m). Stars in (B) and (D) indicate autofluorescent macrophages.

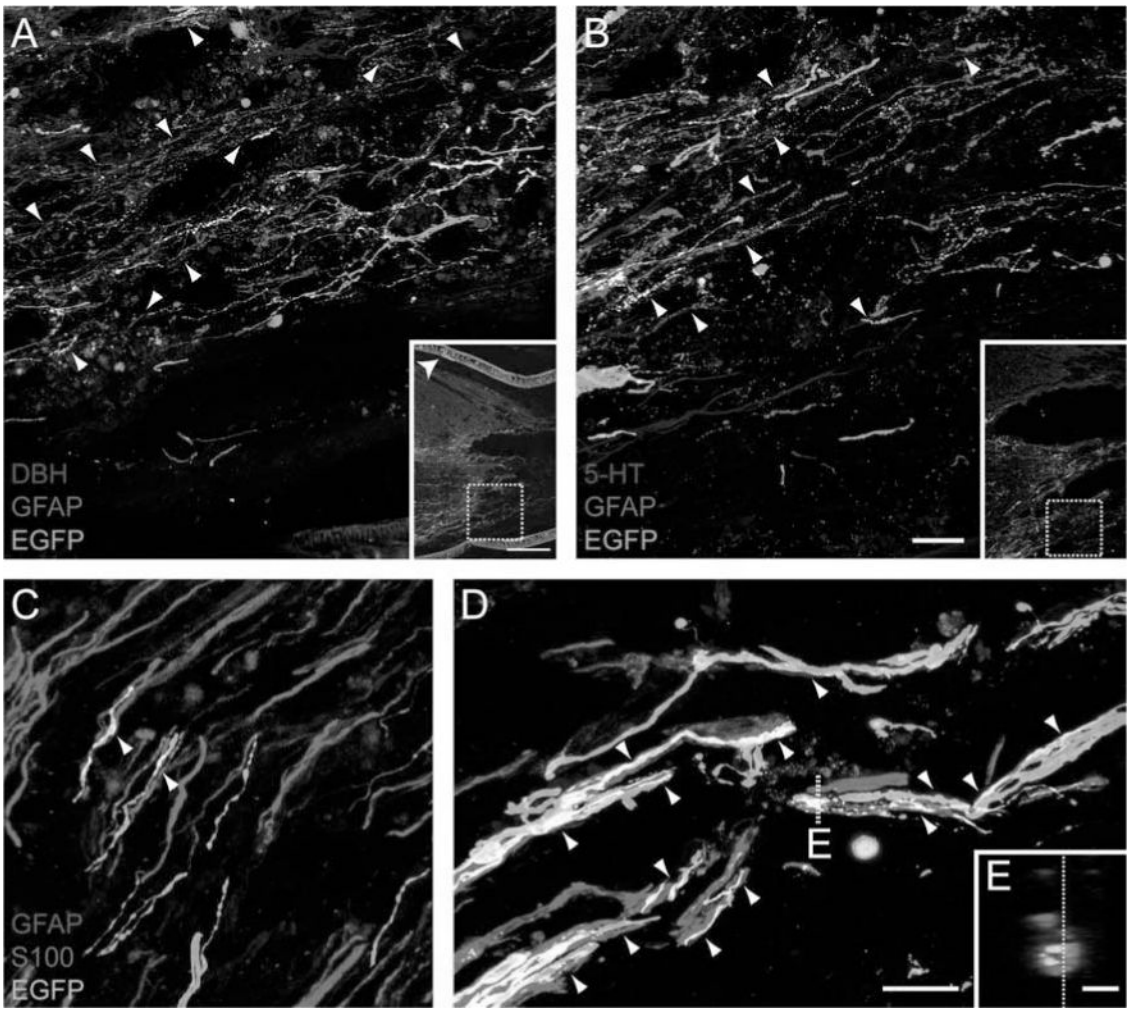

Figure 4.

Following the transplantation of SCs and Matrigel, brainstem axons cross the rostral interface together with GFAP$^+$ astrocyte processes. Both dopamine -hydroxylase-positive (D H$^+$) (red, A) and 5-hydroxytryptophan-positive (5-HT$^+$) (red, B) axons regenerate when GFAP$^+$ (blue) processes form irregular boundaries and elongate into the SC bridge. Arrowheads indicate where GFAP$^+$ processes are in close association with axons. Some axons are yellow/white due to coexpression of either D H or 5-HT with EGFP (green, scale bar: 20 μrn). Insets in (A) and (B) indicate the regions from which the higher magnification images were obtained. The polymer channel is indicated by an arrowhead in the inset in (A) (inset scale bar 200 μm). (C, D) High-magnification confocal images of the rostral interface show the linear and parallel nature of the GFAP$^+$ processes. Arrowheads depict the association of GFAP$^+$ (red) processes, S100$^+$ (blue) SCs, and EGFP$^+$ (green) brainstem axons, which appear white when in close proximity (scale bar: 5 μm). (E) An orthogonal plane of the dashed line in (D) shows SCs and GFAP$^+$ processes bundled together with brainstem axons in the middle (scale bar: 1 μm). The dashed line in (E) indicates the orthogonal plane that was used to obtain the image in (D).

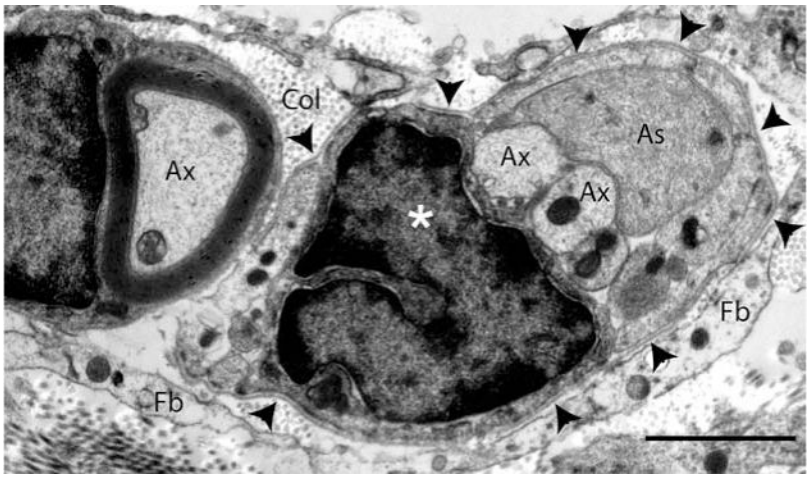

Figure 5.

At the rostral spinal cord/SC bridge interface, axons, SCs, and astrocyte processes are enclosed together within a continuous basal lamina. Six weeks after complete transection and transplantation of an initially fluid SC bridge, this electron micrograph shows axons (Ax), an astrocyte process (As), and a SC nucleus (star), enclosed together within a continuous basal lamina (arrowheads). Cross-sectioned collagen fibers (Col) and fibroblasts (Fb) are visible outside the basal lamina (scale bar: 2 μm). This image was acquired from a cross section of the rostral interface, analogous to the region outlined by box C in Figure 3A.

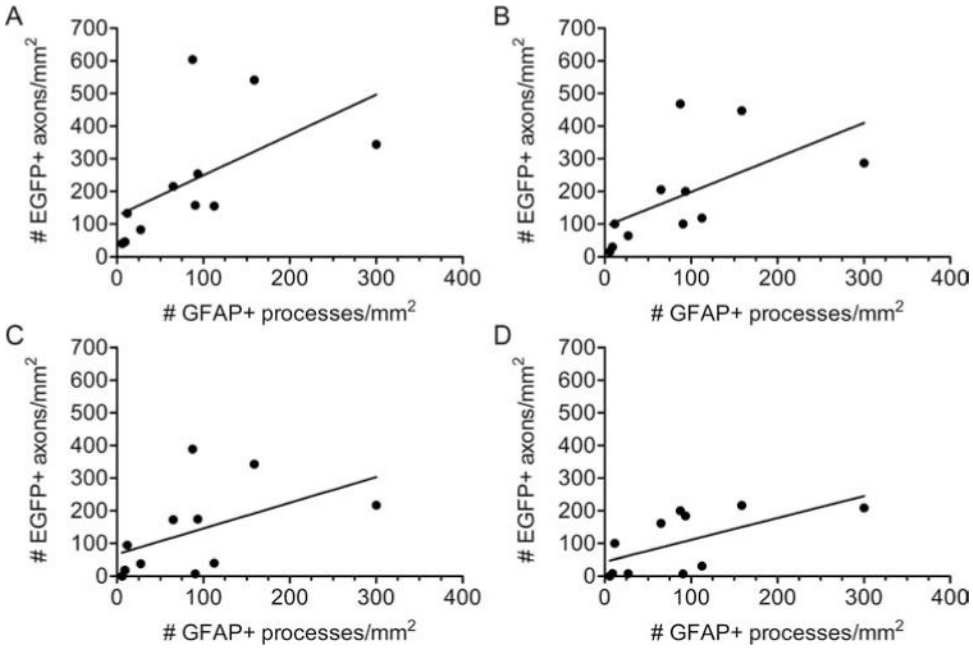

Figure 6.

Increased brainstem axon regeneration is observed when more GFAP$^+$ processes enter a SC bridge. Following transplantation of initially fluid SC bridges, there is a direct correlation between the number of GFAP$^+$ processes that elongate 0.25 mm into the bridge and the number of EGFP$^+$ brainstem axons that regenerate 0.25 mm ($p < 0.005$, $r^2 = 0.31$), (A); 0.5 mm ($p < 0.005$, $r^2 = 0.33$), (B); 1.0 mm ($p < 0.05$, $r^2 = 0.24$), (C); and 1.5 mm ($p < 0.05$, $r^2 = 0.38$), (D).

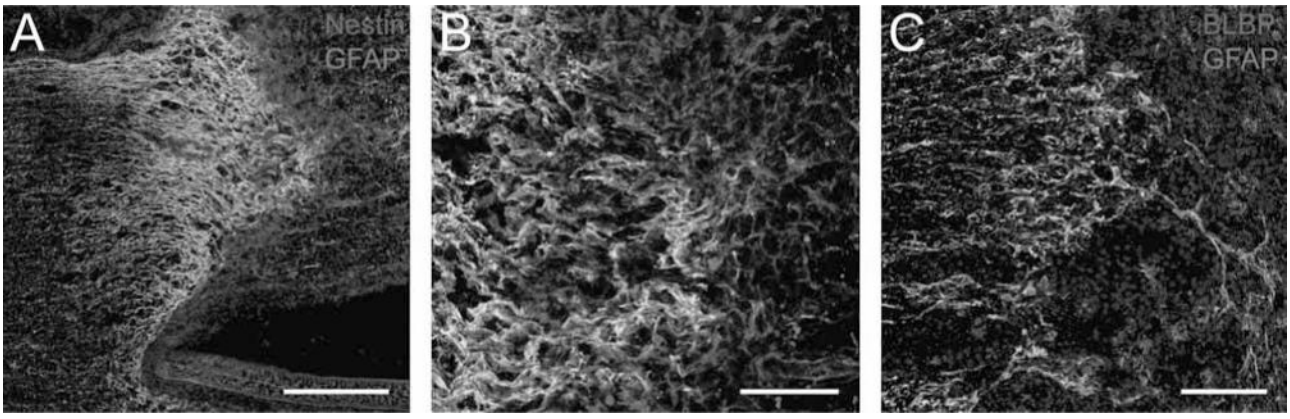

Figure 7.

Astrocyte processes express markers of immature glia at 1 week after transplantation of an initially fluid SC bridge. (A, B) Numerous reactive $GFAP^+$ (green) astrocytes that elongate processes into the bridge also coexpress nestin (red); they appear yellow when coexpressing both proteins at the rostral interface. Many $nestin^+/GFAP^-$ cells (red) are also present beyond the rostral interface and in the SC bridge [scale bar: 250 μm (A), 20 μm (B)]. (C) Numerous $GFAP^+$ (green) astrocytes that elongate processes into the bridge also coexpress brain lipid-binding protein (BLBP; red). $Hoechst^+$ nuclei are blue (scale bar: 50 μm).

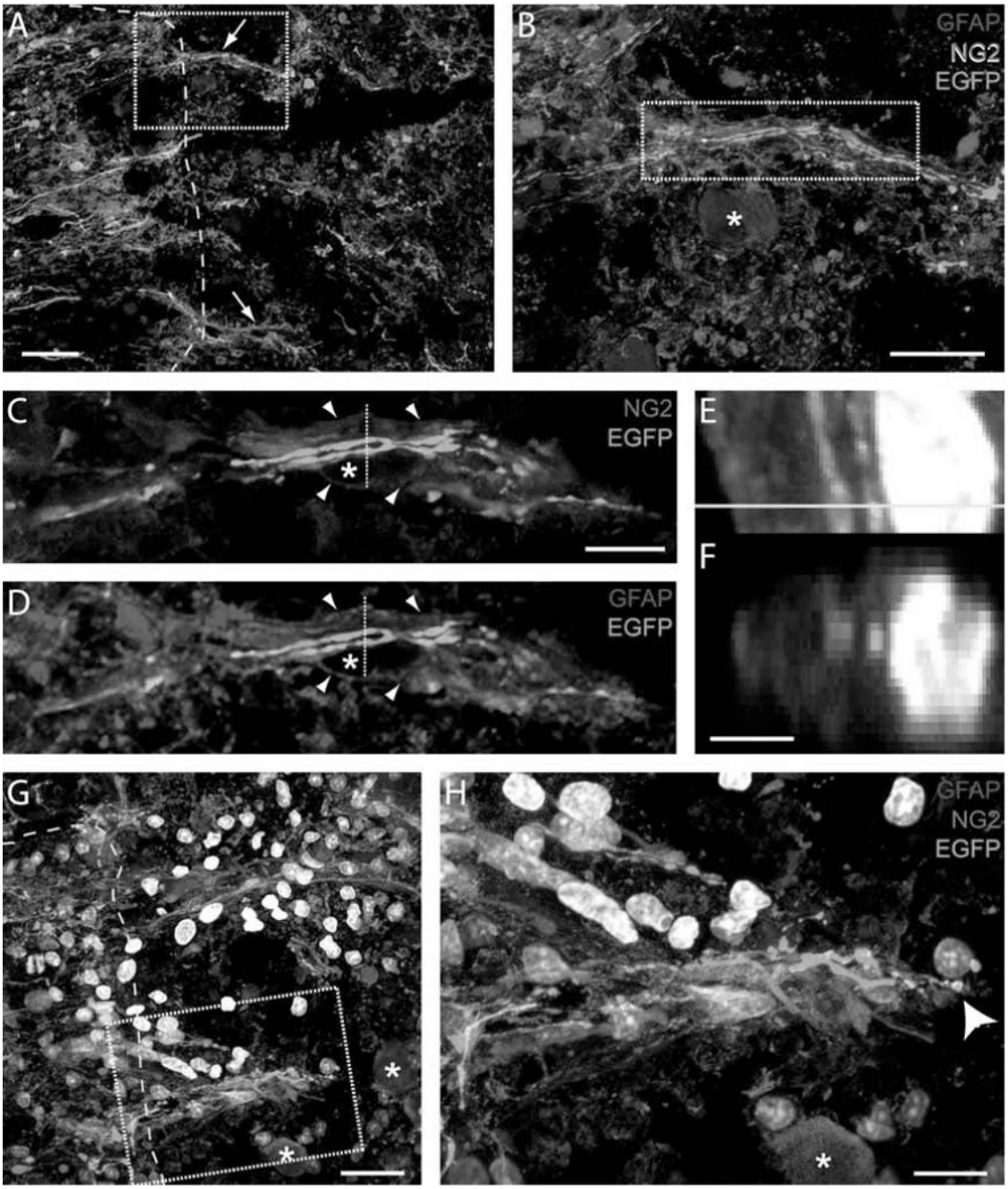

Figure 8.

Brainstem axons regenerate with $NG2^+$/$GFAP^+$ processes following transection and transplantation of an initially fluid SC bridge. (A, B) At 1 week, neuroglycan positive ($NG2^+$) (blue) and $GFAP^+$ (red) processes extend together with $EGFP^+$ (green) brainstem axons beyond the spinal cord boundary (yellow dashed line) and into die bridge (arrows, A). A macrophage nucleus is indicated by a star in (B). The image in (B) is outlined in (A) [scale bars: 20 μm (A), 10 μm (B)]. Single *z*-planes of me region outlined in (B) depict the $EGFP^+$ axons regenerating within $NG2^+$ (C) and $GFAP^+$ (D) tunnels. Arrowheads indicate

the close proximity of NG2 and GFAP expression. Stars indicate the location of a nucleus (scale bar: 5 μm). $EGFP^+$ brainstem axons regenerate among $GFAP^+$ processes (E, F), with NG2 (blue) on me exterior. (F) The orthogonal image of me dashed lines in (C) and (D), and me yellow line in (E). A $Hoechst^+$ nucleus is white (scale bar: 2 μm). (G, H) The tips of $NG2^+/GFAP^+$ processes cross the host spinal cord (yellow dashed line) together with the tips of $EGFP^+$ brainstem axons (arrowhead in H). $Hoechst^+$ nuclei are white. The high-magnification image in (H) is outlined in (G). Adjacent macrophage nuclei are indicated by stars (scale bars: 10 μm and 5 μm, respectively).

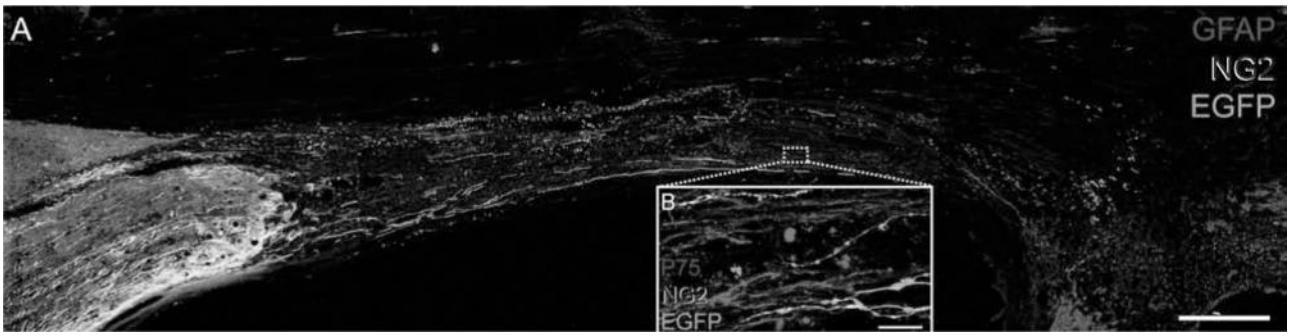

Figure 9.

Six weeks after complete transection, brainstem axons that regenerate into a SC bridge are located in regions of NG2 expression. (A) NG2 (blue) is expressed in linear arrays throughout the SC bridge. $EGFP^+$ (green) brainstem axons regenerate across the entire bridge and are located in regions where NG2 is expressed $GFAP^+$ astrocytes are red (scale bar: 0.5 mm). (B) $EGFP^+$ brainstem axons regenerate in close association with SCs that appear pink due to their coexpression of NG2 (blue) and low-affinity nerve growth factor receptor (p75; red, scale bar: 10 μm).

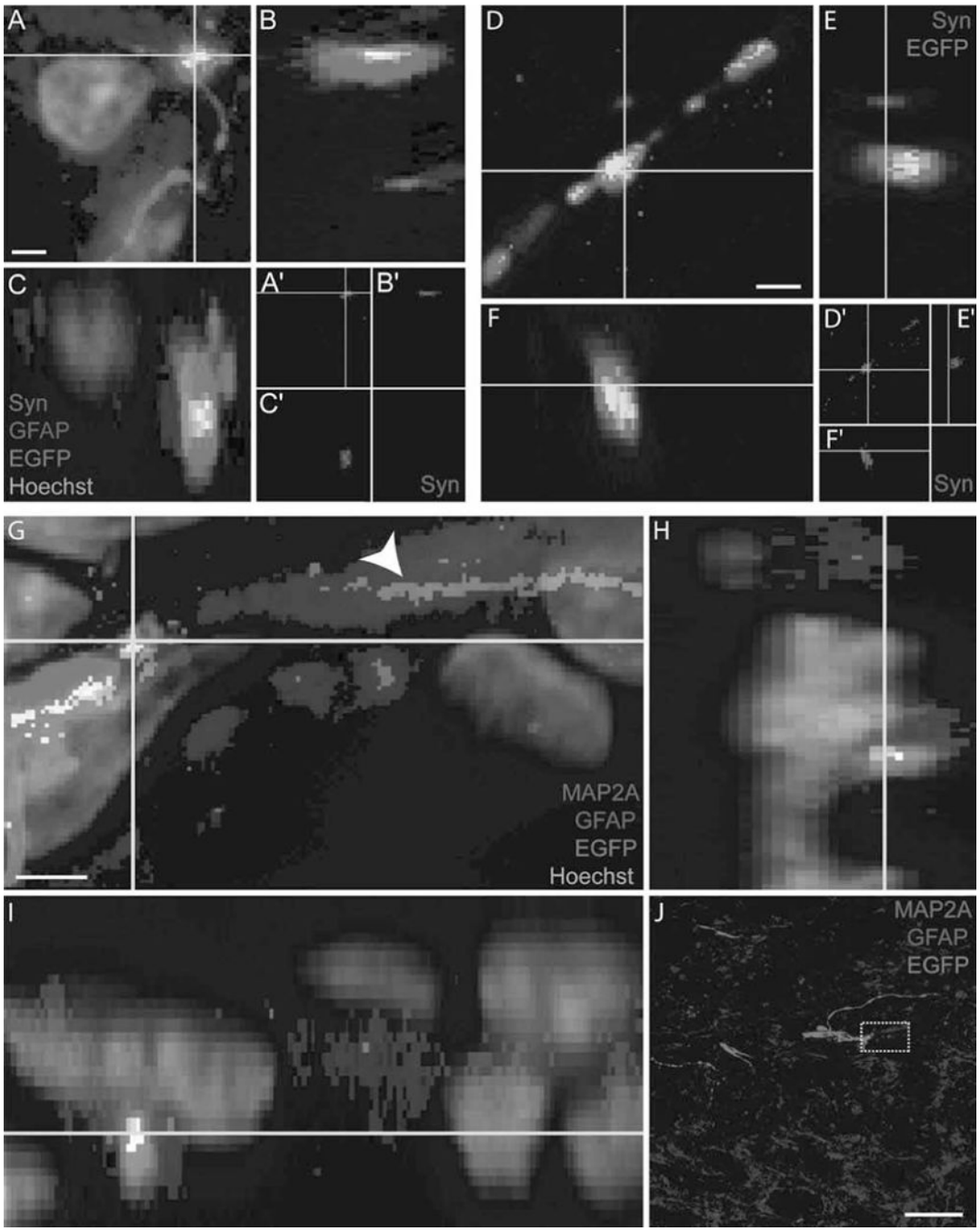

Figure 10.

Regenerating brainstem axons form bouton-like terminals at the caudal interface following transplantation of a SC bridge. (A–C, D–F) EGFP$^+$ (green) brainstem axons that regenerate to the caudal interface form bouton-like terminals and express synaptophysin (Syn; red, A–C, D–F) to create colocalized puncta (yellow). Orthogonal planes are depicted by yellow lines (scale bar: 0.5 ∝m). (G–I) An EGFP$^+$ brainstem axon that regenerates to the caudal interface forms a bouton-like terminal in close association with a microtubule-associated protein 2A-positive (MAP2A$^+$) (red) dendrite. GFAP expression is blue. The dendrite is in

close association with an astrocyte process (arrowhead, G) and juxtaposed in between the $EGFP^+$ axon and astrocyte process (yellow/white, G–I). Orthogonal planes are depicted by yellow lines (scale ban 0.5 ∝m). (J) Low magnification of the caudal interface, the region where the images in (G–I) were obtained are indicated by a dashed box (scale bar: 20 μm).

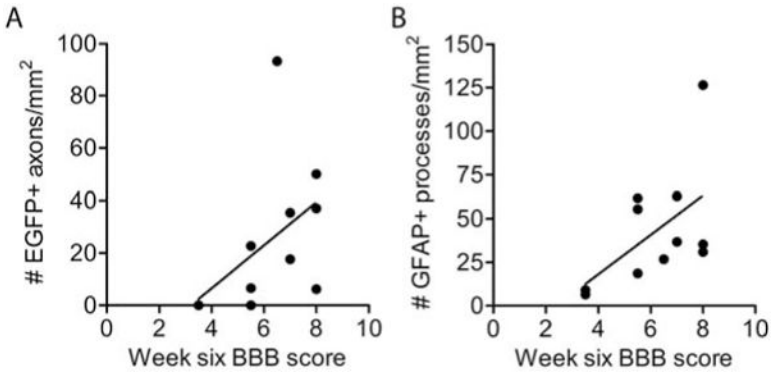

Figure 11.

Both brainstem axon regeneration and the elongation of GFAP$^+$ processes correlate with improvement in hindlimb movement following transplantation of an initially fluid SC bridge. (A) The number of EGFP$^+$ axons/mm^2 that reach the caudal interface (0 in Fig. 1A) directly correlates with improvement in hindlimb locomotion test scores (BBB, $p<0.05$, $r^2 = 0.22$, $n= 11$, two animals scored 3.5). (B) The total number of GFAP$^+$ processes at 0.25 mm, 0.5 mm, and 1.0 mm beyond both the rostral and caudal interfaces was determined for each animal. The number of GFAP$^+$ processes/mm^2 in the SC bridge directly correlates with improvement in hindlimb locomotion test scores (BBB, $p < 0.05$, $r^2 = 0.3$).